The EMBO Journal (2013) 32, 829–843
www.embojournal.org

TRANSPARENT PROCESS

THE EMBO JOURNAL

A role for LFA-1 in delaying T-lymphocyte egress from lymph nodes

Peter Reichardt[1,4], Irene Patzak[2,4], Kristian Jones[2], Eloho Etemire[3], Matthias Gunzer[1,3,5] and Nancy Hogg[2,5,*]

[1]Institute of Molecular and Clinical Immunology, Otto von Guericke University Magdeburg, Magdeburg, Germany, [2]Leukocyte Adhesion Laboratory, Cancer Research UK London Research Institute, London, UK and [3]University Duisburg/Essen, Universitätsklinikum Essen, Institute of Experimental Immunology and Imaging, Hufelandstraße 55, Essen, Germany

Lymphocytes use the integrin leukocyte function-associated antigen-1 (LFA-1) to cross the vasculature into lymph nodes (LNs), but it has been uncertain whether their migration within LN is also LFA-1 dependent. We show that LFA-1 mediates prolonged LN residence as *LFA-1*$^{-/-}$ CD4 T cells have significantly decreased dwell times compared with *LFA-1*$^{+/+}$ T cells, a distinction lost in hosts lacking the major LFA-1 ligand ICAM-1. Intra-vital two-photon microscopy revealed that *LFA-1*$^{+/+}$ and *LFA-1*$^{-/-}$ T cells reacted differently when probing the ICAM-1-expressing lymphatic network. While *LFA-1*$^{+/+}$ T cells returned to the LN parenchyma with greater frequency, *LFA-1*$^{-/-}$ T cells egressed promptly. This difference in exit behaviour was a feature of egress through all assessed lymphatic exit sites. We show that use of LFA-1 as an adhesion receptor amplifies the number of T cells returning to the LN parenchyma that can lead to increased effectiveness of T-cell response to antigen. Thus, we identify a novel function for LFA-1 in guiding T cells at the critical point of LN egress when they either exit or return into the LN for further interactions.

The EMBO Journal (2013) **32,** 829–843. doi:10.1038/emboj.2013.33; Published online 26 February 2013
Subject Categories: signal transduction; immunology
Keywords: LFA-1; lymphatics; lymph node; migration; T cells

Introduction

The integrin leukocyte function-associated antigen-1 (LFA-1; αLβ2; CD11a/CD18) contributes to lymphocyte adhesion and migration in two major ways. It orchestrates adhesive interactions between T and B lymphocytes and their antigen-presenting cells (APC) thereby lowering the threshold for stimulation during immune responses (Grakoui *et al*, 1999; Carrasco *et al*, 2004). LFA-1 is also vital for the continual migration of lymphocytes across high endothelial venules (HEVs) into lymph nodes (LNs) and into other tissues during an infection (Hamann *et al*, 1988; Berlin-Rufenach *et al*, 1999). Entering an LN is a multistep process that includes signalling into lymphocytes by endothelial-tethered chemokines (von Andrian and Mempel, 2003; Bajenoff *et al*, 2007; Evans *et al*, 2009; Girard *et al*, 2012). This initiates the process of LFA-1 activation, firm binding of lymphocytes and their subsequent migration across the vasculature into the LN parenchyma. An unresolved question is whether LFA-1 exclusively mediates immigration into the LN or, in the absence of antigen, also has a role in leukocyte trafficking within the node itself. In favour of integrin-independent migration are studies with 'integrin nude' dendritic cells (DCs) that migrate normally *in vivo* (Lammermann *et al*, 2008). In contrast, *CD18*$^{-/-}$ T cells move in the T zone of the LN with 15% lower velocity than WT T cells (Woolf *et al*, 2007).

T lymphocytes continually leave the circulation and spend 6–12 h within an LN where they may encounter APC in keeping with their role in immune surveillance (Smith and Ford, 1983; Tomura *et al*, 2008). The LN is a lymphocyte-filled structure consisting of dense T and B cell-dominated areas, each with a network of potentially antigen-loaded conduits and presenting cells along which the lymphocytes migrate (Gretz *et al*, 2000; Sixt *et al*, 2005; Bajenoff *et al*, 2006). T cells exit the LN via the lymphatic vessel (LV) network composed of the subcapsular sinus that connects with the T zone adjacent cortical sinuses and the macrophage-rich medulla. Recent reports show that T cells can exit into the LVs from all these locations within the node (Grigorova *et al*, 2009; Sinha *et al*, 2009). Their departure from the LN depends on competition between the CCL19/CCL21 chemokine receptor CCR7 that delivers a retention signal and the sphingosine 1-phosphate receptor-1 (S1P1) that increases in expression over time that the T cells spend in the LN (Lo *et al*, 2005; Pham *et al*, 2008). Interaction of S1P1 with its ligand sphingosine 1-phosphate (S1P) on the lymphatic endothelium is considered to constitute a directional signal for T-cell egress (Grigorova *et al*, 2009). As a final step, the lymphocytes are transported by the lymphatic drainage into blood via the thoracic duct (Gowans, 1957).

We show by adoptive transfer and intra-vital two-photon microscopy that *LFA-1*$^{-/-}$ T cells pass through the LN more rapidly than *LFA-1*$^{+/+}$ T cells and that LFA-1 is not essential for T-cell egress. In contrast, LFA-1-expressing T cells are restrained on the lymphatic vasculature and re-visit the LN parenchyma with greater frequency rather than exiting immediately. This leads to a more effective priming of adoptively transferred T cells in WT LNs, compared with *ICAM-1*$^{-/-}$ LNs. Thus, we identify LFA-1 as a critical adhesion factor influencing the fate of T cells at the point of LN exiting.

*Corresponding author. Cancer Research UK London Research Institute, Leukocyte Adhesion Laboratory, 44 Lincoln's Inn Fields, London WC2A 3LY, UK. Tel.: +44 207 269 3255; Fax: +44 207 269 3417;
E-mail: nancy.hogg@cancer.org.uk
[4]Joint First Authors.
[5]Joint Senior Authors.

Received: 20 August 2012; accepted: 31 January 2013; published online: 26 February 2013

Results

Transit of LFA-1$^{-/-}$ and LFA-1$^{+/+}$ T lymphocytes through the inguinal LN

To assess whether the major subset of recirculating CD4 T cells use LFA-1 as they travel through a LN, we compared the intra-nodal behaviour of *LFA-1*$^{-/-}$ and *LFA-1*$^{+/+}$ T cells. The two CD4 T-cell populations expressed comparable proportions of CD44^{lo} and CD62L^{high} markers typical of recirculating naïve cells that have not been exposed to antigen (WT, 68.5 ± 3.66%; KO, 75.63 ± 3.02% (mean ± s.e.m.), $n = 6$ mice, $P = 0.163$), with the remainder representing a more mature CD44^{high} and CD62L$^{lo\text{-}int}$ CD4 T-cell phenotype (Supplementary Figure 1A). Thus, lack of LFA-1 did not affect T-cell maturation in terms of proportions of naïve and non-naïve CD4 T cells.

Following differential labelling using either fluorescent green CSFE or orange SNARF-1 dyes, we injected purified CD4 T cells in equivalent numbers into the tail vein of host WT mice as previously described (Berlin-Rufenach *et al*, 1999). The adoptively transferred CD4 T cells revealed a uniform phenotype of CD44^{lo} and CD62L^{int}, typical of intra-nodal naïve T cells (WT, 93.2 ± 0.92%; KO, 95.2 ± 0.95% (mean ± s.e.m.), $n = 4$ mice/group, $P = 0.335$) (Supplementary Figure 1B; Klinger *et al*, 2009). Pre-sorting CD4 and CD44^{lo} T cells yielded a similar result (data not shown).

At 6 h when both entry into and egress from the inguinal LN was occurring, the ratio of *LFA-1*$^{+/+}$ over *LFA-1*$^{-/-}$ CD4 T cells was ~7:1 (WT/KO, 6.8 ± 1.5) (mean ± s.d.) (Figure 1A; Smith and Ford, 1983; Tomura *et al*, 2008). To focus exclusively on the behaviour of T cells already in the LN, we blocked further entry at 6 h using a combination of MEL-14 and PS2/3 mAbs specific for L-selectin and α4 integrin, adhesion receptors that have critical roles in lymphocyte LN entry along with LFA-1. In control contemporaneous experiments, we showed that the mAb-blocking regime equivalently prevented entry of *LFA-1*$^{+/+}$ and *LFA-1*$^{-/-}$ T cells into the inguinal LN (WT block—98.9 ± 0.4%, KO block—99.4 ± 0.3% (mean ± s.e.m.), $n = 3$ mice per group) (Supplementary Figure 1C). Following this blockade, the WT/KO ratio was altered 4–6 h later to ~16:1 (10 h: WT/KO, 15.7 ± 5.0; 12 h: WT/KO, 17.5 ± 4.5) (mean ± s.d.) (Figure 1A). It was important to establish that the adoptively transferred *LFA-1*$^{+/+}$ and *LFA-1*$^{-/-}$ T cells were equally viable between 6 and 10 h (Annexin V staining, data not shown). Thus, the 2.3-fold increase in WT/KO ratio suggested that *LFA-1*$^{-/-}$ T cells passed through the LN at a faster rate than *LFA-1*$^{+/+}$ T cells.

To further confirm that it was absence of LFA-1 itself that was responsible for the altered LN trafficking, we decreased the advantage of *LFA-1*$^{+/+}$ over *LFA-1*$^{-/-}$ CD4 T cells by transferring both T-cell types into host mice deficient in the most widespread LFA-1 ligand, ICAM-1 (Figure 1B). In this situation, the initial ratio of *LFA-1*$^{+/+}$ to *LFA-1*$^{-/-}$ T cells was similar to the WT hosts as *LFA-1*$^{+/+}$ T cells can make use of a second LFA-1 ligand, ICAM-2, to cross the HEV (Boscacci *et al*, 2010). Following mAb blockade at 6 h of further T-cell LN entry into *ICAM-1*$^{-/-}$ host mice, the WT/KO ratio did not however significantly change at 10 h (6 h: WT/KO, 5.4 ± 1.2; 10 h: WT/KO, 3.5 ± 0.2 (mean ± s.d.)) unlike the situation in the WT host (Figure 1B). This provided more evidence that it was lack of LFA-1 and not some other developmental feature of *LFA-1*$^{-/-}$ T cells that was responsible for the accelerated journey of the T cells through the LN.

We next asked whether T-cell access to the different compartments of the LN was LFA-1 dependent and would provide an explanation for the more rapid LN journey of *LFA-1*$^{-/-}$ T cells. Adoptively transferred *LFA-1*$^{+/+}$ and *LFA-1*$^{-/-}$ CD4 T cells were both observed to be widespread in the T-cell parenchymal areas at 6 h after T-cell transfer, ranging from the peripheral areas bordering the B-cell follicles (inset 1) to the dense T-cell zone (inset 2) (Figure 1C). An average of 95.7 ± 16.6 *LFA-1*$^{+/+}$ and *LFA-1*$^{-/-}$ 16.7 ± 2.8 T cells was counted in LN sections of the T-cell zone (mean ± s.e.m. of individual LN tissue slices from 7 host mice) giving a ratio of 7/1, which is identical to the ratio obtained by flow cytometry of whole LNs.

Although lack of LFA-1 expression did not prevent T cells from accessing the T-cell zone, it might influence the characteristics of their migration. Investigating the motility of the two types of cells using intra-vital two-photon microscopy within the T zone, we found that *LFA-1*$^{+/+}$ T cells were 11% faster than *LFA-1*$^{-/-}$ T cells (WT, 12.30 ± 0.49 μm/min versus KO, 10.82 ± 0.44 μm/min (mean ± s.e.m), $P < 0.02$) (Figure 1D). There was no significant difference in their migration in *ICAM-1*$^{-/-}$ hosts (WT, 9.84 ± 0.55 μm/min versus KO, 8.62 ± 0.41 μm/min, $P = 0.08$) (Figure 1D). This further confirmed that the effect on migration was LFA-1 regulated by binding of LFA-1 to ICAM-1.

In summary, *LFA-1*$^{-/-}$ CD4 T cells had a shorter dwell time in the LN than *LFA-1*$^{+/+}$ T cells implying that the latter cells were being restrained through interaction via LFA-1. The fact that *LFA-1*$^{+/+}$ T cells had slightly increased speed compared with *LFA-1*$^{-/-}$ T cells in the T zone did not obviously account for their apparently longer time in the LN. Importantly, the difference in travel time was abolished when *LFA-1*$^{+/+}$ T cells were adoptively transferred into *ICAM-1*$^{-/-}$ hosts where they behaved like *LFA-1*$^{-/-}$ T cells.

Accumulation of LFA-1$^{+/+}$ T cells compared with LFA-1$^{-/-}$ T cells at LYVE-1-expressing LVs

A possible explanation for the difference between *LFA-1*$^{+/+}$ and *LFA-1*$^{-/-}$ T cells in the timing of LN residence might depend on a differential ability to leave the LN via the draining lymphatic vasculature. To directly test this possibility, we investigated T-cell associations with the LV by intra-vital two-photon imaging of the inguinal LN from its hilar side towards the follicular side up to a depth of ~150 μm. It was possible to compare areas of the T zone that were LV free as well as distinct LV-containing areas. Within the latter, we observed centrally located, T zone-adjacent LV areas (central, cLV) where the network of LV was tubular in shape and without any macrophage association and more peripherally located LV areas (peripheral, pLV) towards the medullary region, where the tubular LV became increasingly lined with macrophages (Miller *et al*, 2002; Matheu *et al*, 2011) (Figure 2A; Supplementary Figure S2A).

The overall density of adoptively transferred T cells in these two areas was similar (cLV, 26.8 ± 6.4 total T cells/field of view; pLV, 29.0 ± 12.9 total T cells/field of view). However, the important finding was that the ratio of *LFA-1*$^{+/+}$/*LFA-1*$^{-/-}$ T cells in both of the LV-dominated regions was enhanced by ~50% compared with the proper T zone (ratio in T zone set at 1:0 for comparison purposes) (Figure 2B). This greater

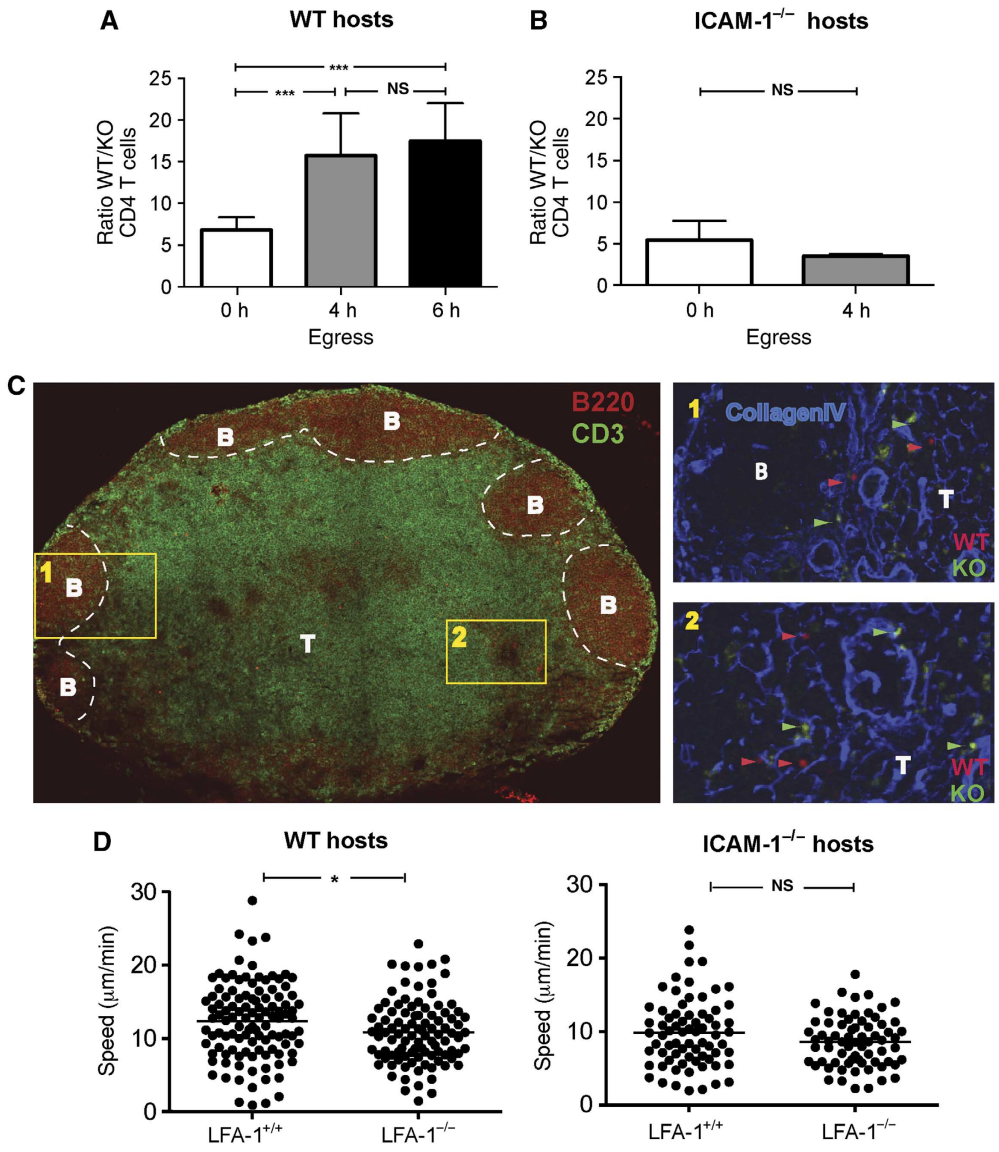

Figure 1 Comparison of non-stimulated *LFA-1*$^{+/+}$ and *LFA-1*$^{-/-}$ CD4 T-lymphocyte behaviour in the inguinal LN. (**A**) The numbers of CD4 T cells in host mice expressed as a ratio of *LFA-1*$^{+/+}$ (WT) to *LFA-1*$^{-/-}$ (KO) over time; CFSE and SNARF-1-labelled CD4 T cells (5×10^6 per cell type) were adoptively transferred into WT host mice and the T cells present in the LN at 6, 10 and 12 h were quantified; further entry was blocked from 6 h onwards with anti-L-selectin and α4 mAbs; each data point represents ⩾7 mice. (**B**) Experimental set-up as in (**A**), but with *ICAM-1*$^{-/-}$ mice used as adoptive transfer hosts. The ratio of WT/KO CD4 T cells at 6 and 10 h is shown; $n = 9$ mice per time point. (**C**) Tiled image showing immunostained CD3$^+$ T-cell area (green) and B220$^+$ B-cell follicles (red). Insets show the distribution at 6 h following transfer of *LFA-1*$^{+/+}$ T cells (WT, red), *LFA-1*$^{-/-}$ T cells (KO, green) and collagen IV (blue) at the T-/B-cell boundary (inset 1) and the deep T-cell zone (inset 2). The images are representative of six tissue slices from three mice. (**D**) Motility of *LFA-1*$^{-/-}$ and *LFA-1*$^{+/+}$ CD4 cells in T-cell zone in WT and *ICAM-1*$^{-/-}$ host mice in the T zone at 150 μm depth; velocity data from intra-vital two-photon imaging combined from three experiments with >100 cells analysed per host mouse strain.

LV-associated accumulation of *LFA-1*$^{+/+}$ T cells was lost when *ICAM-1*$^{-/-}$ mice were used as hosts further confirming a key role for LFA-1 in this skewed distribution (Figure 2C).

Collectively, the analysis of T-cell distribution within the LN revealed that *LFA-1*$^{+/+}$ T cells were more extensively represented than *LFA-1*$^{-/-}$ T cells in the regions where LV pre-dominated. As this effect was dependent on ICAM-1, LFA-1 appeared to affect the behaviour of T cells at the LV via ICAM-1 interactions.

Expression of ICAM-1 by LVs

An important issue was whether LYVE-1$^+$ LV directly expressed the most widespread LFA-1 interaction partner, ICAM-1, under non-inflammatory conditions. A broad pattern of ICAM-1 staining was observed on LN tissue sections with labelling of macrophages, DCs, fibroblastic cells, and endothelial cells as previously described (Katakai *et al*, 2004; Westermann *et al*, 2005; Woolf *et al*, 2007). We also observed significant ICAM-1$^+$ staining that colocalised with LYVE-1$^+$ LV in both the central (*inset 1*) and peripheral (*inset 2*) regions of the LN (Figure 3A). To quantify the coincidence in expression of LYVE-1 and ICAM-1 on the LVs, we randomly selected LV and performed pixel-by-pixel comparison of LYVE-1 and ICAM-1 staining (Figure 3B). The overlap in staining indicated substantial co-expression (central LV: 72.93 ± 1.75%; peripheral LV: 80.26 ± 3.0%; isotype control: 1.2 ± 0.4% (mean ± s.d.)).

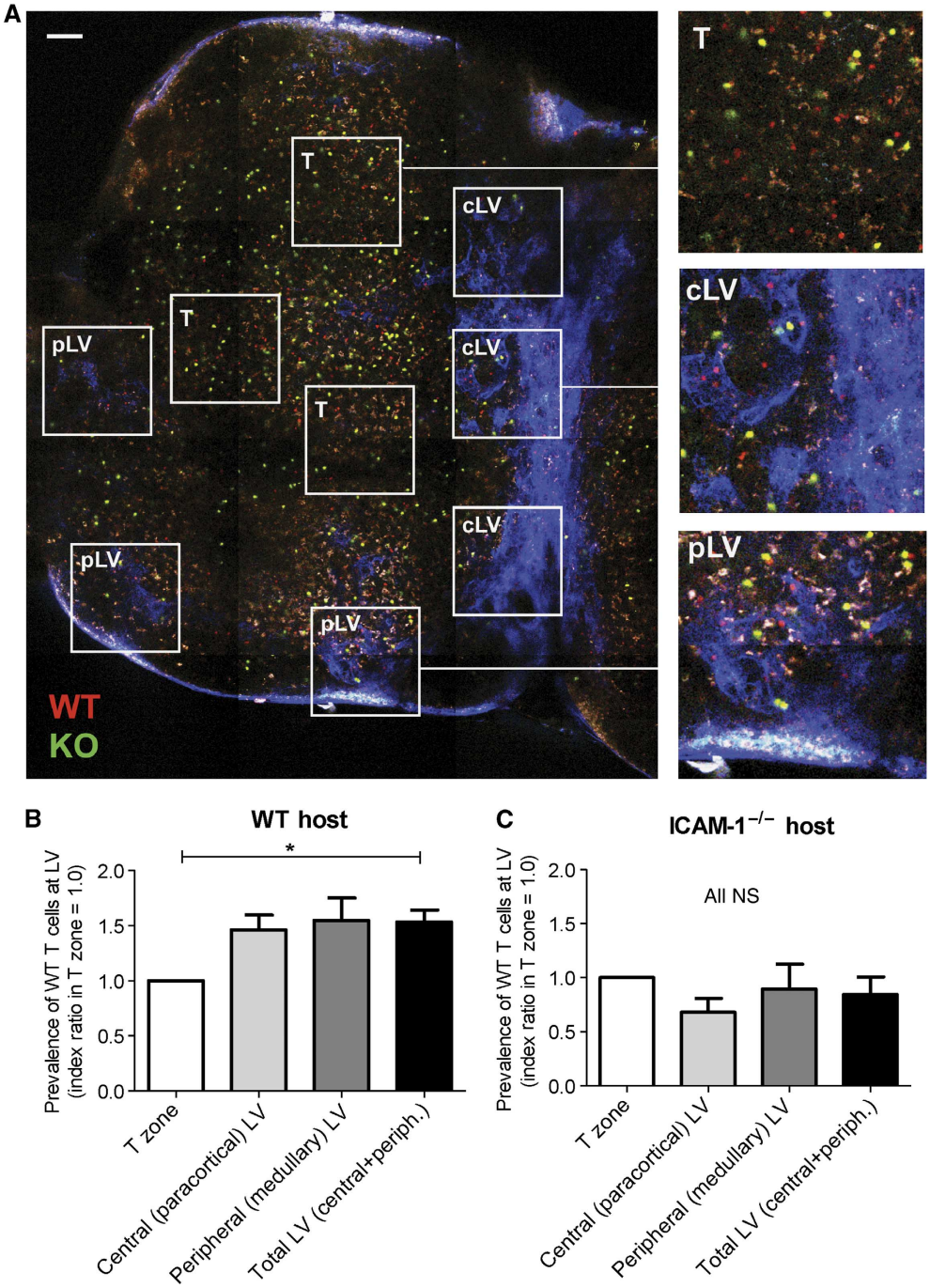

Figure 2 Distribution of *LFA-1*$^{+/+}$ and *LFA-1*$^{-/-}$ T cells in T zone and peripheral regions of the LN. (**A**) Tiled image of an explanted inguinal LN showing three distinct zones used for quantification of the *LFA-1*$^{+/+}$/*LFA-1*$^{-/-}$ T cell (WT/KO) ratio; scale bar = 100 μm. Insets for each zone as typically quantified for analysis are shown: the T-cell zone (T zone, >150 μm depth); central zone (cLV) at 80–150 μm depth showing LYVE-1^{+} lymphatic vessels (blue); peripheral medullary region (pLV) at 50–80 μm depth showing LYVE-1^{+} LV (blue) ± associated autofluorescent macrophages (white). (**B**) Increased prevalence of *LFA-1*$^{+/+}$ over *LFA-1*$^{-/-}$ T cells in the central and peripheral LV-associated regions over the T zone (set at an index ratio of 1.0) in WT host mice; data are averaged from four experiments with a total of >600 T cells analysed. (**C**) Lack of increased prevalence of *LFA-1*$^{+/+}$ over *LFA-1*$^{-/-}$ T cells in central and peripheral type LV-associated regions over T zone in host *ICAM-1*$^{-/-}$ mice; data are averaged from three experiments with >500 T cells analysed.

These findings established that the LV of unimmunised mice expresses the LFA-1 ligand ICAM-1 *in situ*, thus providing interaction opportunities for LFA-1-expressing T cells.

LFA-1$^{+/+}$ *and LFA-1*$^{-/-}$ *T cells differ in terms of ICAM-1-dependent migration to chemokine CCL21 and S1P*

As critical interplay between receptors CCR7 and S1P1 governs T-cell exit into the LV (Lo *et al*, 2005; Pham *et al*, 2008; Grigorova *et al*, 2009), a difference in migratory response to the key mediators CCL21 and S1P might explain the behaviour of *LFA-1*$^{-/-}$ compared with *LFA-1*$^{+/+}$ T cells. Western blotting indicated that their receptors S1P1 and CCR7 were equally expressed in terms of total receptor amounts by the two T cell types (Figure 4A) and CCR7 was detected equivalently at membrane level as determined by FACS analysis (WT, 4745 ± 2285 versus KO, 4482 ± 2264

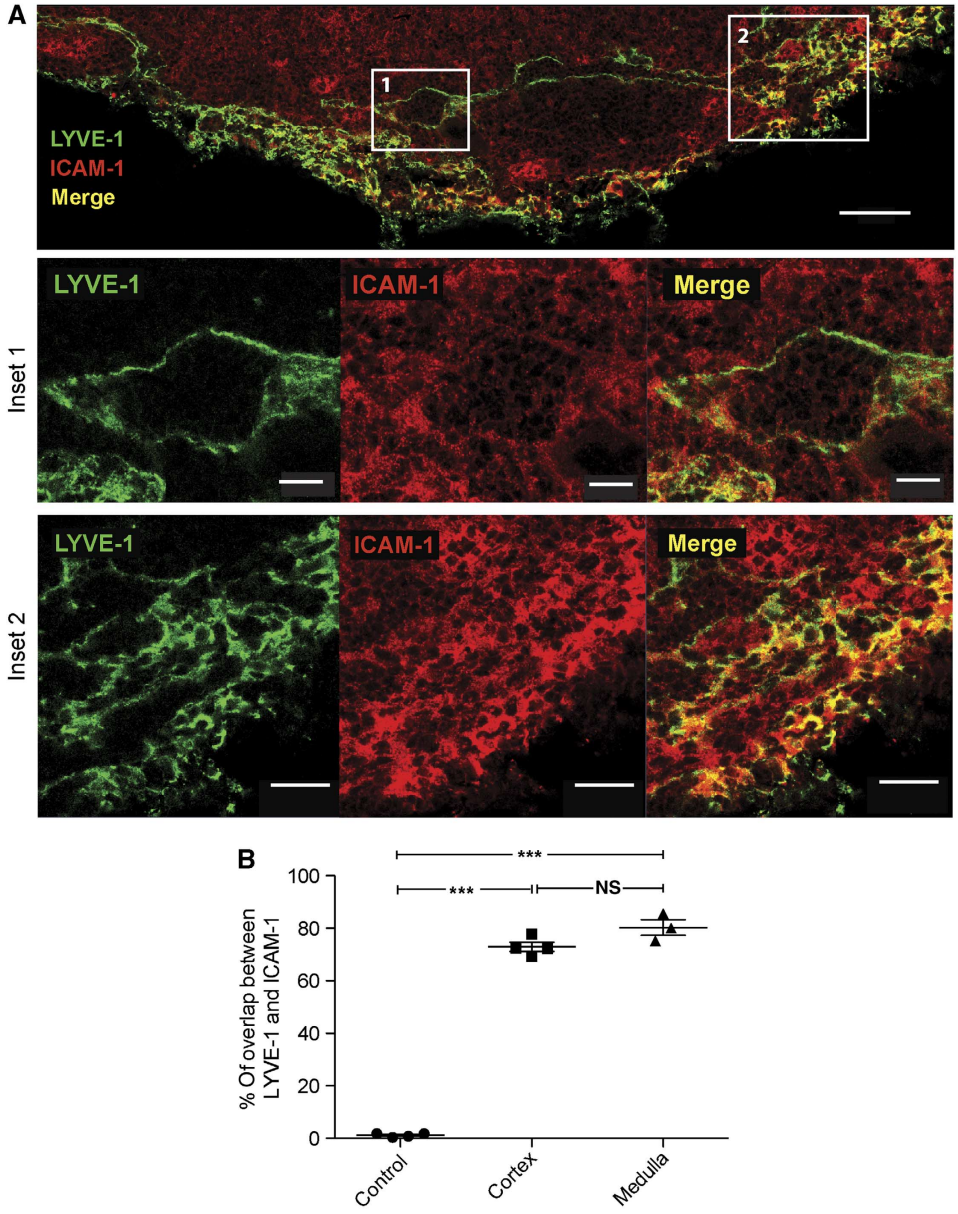

Figure 3 Co-expression of ICAM-1 and LYVE-1 on the lymphatic vasculature. (**A**) Immunohistochemical images of an unstimulated inguinal pLN tissue section comparing LYVE-1 (green) LV with ICAM-1 (red) and merged (yellow) staining; scale bar = 50 μm. Shown enlarged below: inset 1 indicates a T zone-associated LV and inset 2, a peripheral LV region; scale bars 10 and 20 μm, respectively. (**B**) Pixel-by-pixel determination of the overlap in staining between LYVE-1 and ICAM-1 on LV; data were generated from tissue sections of seven LNs. An isotype control mAb for ICAM-1 was also compared with LYVE-1 mAb and showed no staining or overlap; tissue sections from three LNs.

(mean fluorescence intensity ± s.d.)) (Figure 4B). We next tested the T cells for their ability to undergo migration to S1P and CCL21 using a transwell chemotaxis assay under ICAM-1-independent (Figure 4C) or ICAM-1-dependent conditions (Supplementary Figure 3). Under these circumstances, *LFA-1*$^{-/-}$ as well as *LFA-1*$^{+/+}$ T cells responded positively to the mediators and in a similar fashion whether or not ICAM-1 was present. Finally, we measured the response to S1P and CCL21 in a shear flow assay where engaging immobilised ICAM-1 and stimulants was necessary for adhesion and migration. Under these conditions only *LFA-1*$^{+/+}$ T cells, but not *LFA-1*$^{-/-}$ T cells, were able to attach and migrate to both S1P and CCL21 (Figure 4D).

Although these *in vitro* experiments showed *LFA-1*$^{-/-}$ and *LFA-1*$^{+/+}$ T cells to be migrating similarly in response to S1P, a question was whether the motility difference observed *in vivo* was dependent upon responsiveness toward S1P within the node. However, treatment of mice with FTY720, the general downregulator of S1P receptor that causes blockade of T-cell egress from the pLN, did not alter the velocity differential between *LFA-1*$^{+/+}$ and *LFA-1*$^{-/-}$ CD4 T-cell motility within the LN (Supplementary Figure 4).

These experiments showed that signalling through CCR7 and S1P1 on the CD4 T cells was not altered by LFA-1 deficiency. Additionally, both mediators had the ability to activate LFA-1 adhesion/migration under shear flow conditions. This differential adhesion to ICAM-1 could also be a factor determining T-cell behaviour *in vivo* and, when happening at ICAM-1-expressing LV, might be expected to influence their egress.

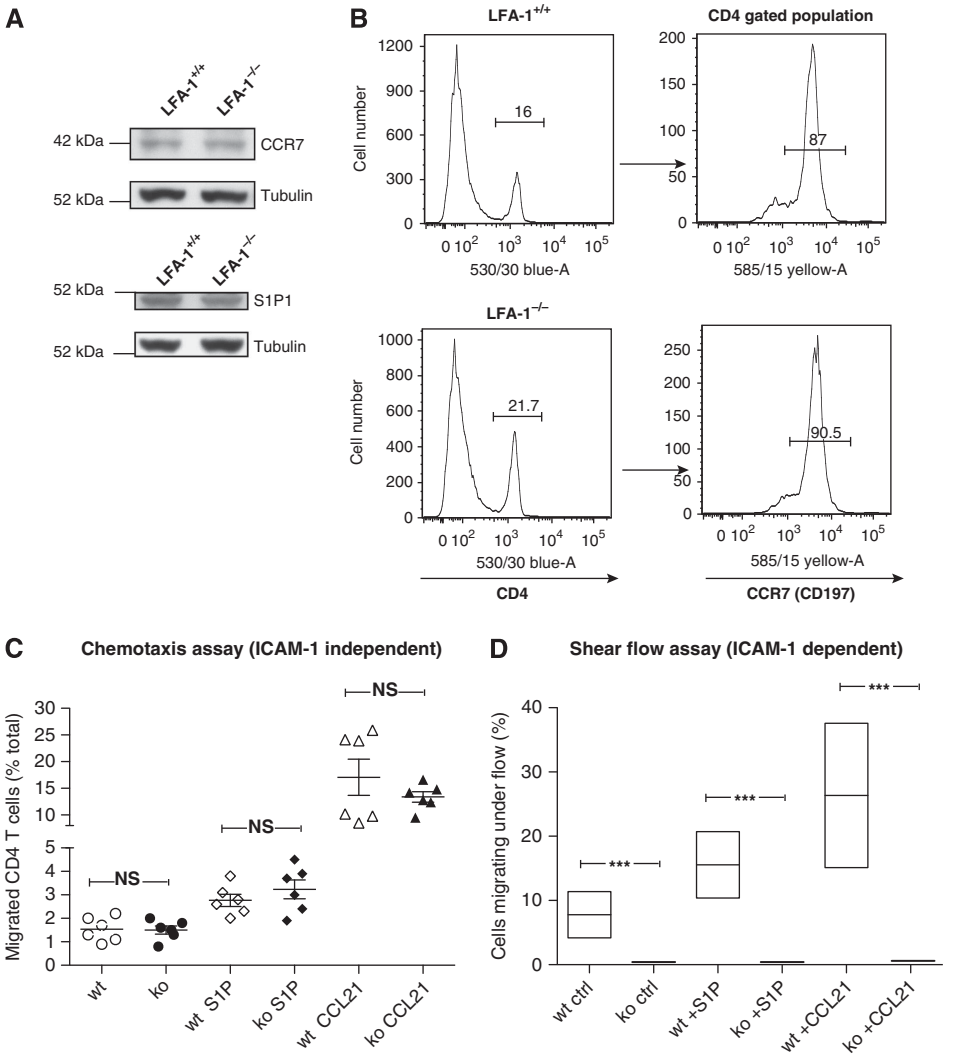

Figure 4 Responses of *LFA-1*$^{+/+}$ and *LFA-1*$^{-/-}$ CD4 T cells to S1P and CCL21. (**A**) Western blotting analysis of CCR7 and S1P1 (EDG-1) levels in CD4 T cells with α-tubulin serving as a sample loading control; data are typical for $n = 2$ experiments. (**B**) Flow cytometry analysis indicating the proportions of *LFA-1*$^{+/+}$ and *LFA-1*$^{-/-}$ CD4 lymphocytes in LN and splenocyte sample and the proportion of each that expressed CCR7; typical result of $n = 2$. (**C**) Transwell assay on uncoated filters showing the percentage of total input T cells that responded to 25 nM S1P and 6 μM CCL21 in the lower chamber; data averaged from $n = 6$ assays. (**D**) Shear flow assay showing proportion of total T cells in contact with ICAM-1 that adhered and migrated under flow conditions of 1 dyne cm^2 in response to S1P and CCR7 as above; $n = 90$–120 T cells were analysed per condition; $n = 3$ experiments.

LFA-1$^{+/+}$ *and LFA-1*$^{-/-}$ *T-cell associations with central LVs adjacent to the T zone*

We next studied the motile behaviour of T cells in regions with LYVE-1$^+$ LVs. In general, the T cells within the paracortical region were observed to migrate with higher motility than the T cells at the periphery of the T zone (Supplementary Video 1). The spread of high MW FITC dextran indicated that the flow of lymphatic fluid throughout the network was intact during the investigation (Supplementary Figure S2B; Gretz *et al*, 2000). This was further corroborated by observing persistent lymphatic flow during the whole imaging period as detected in an efferent vessel over 2 h (Supplementary Video 2).

The LVs in the paracortical area were characteristically tubular shaped and devoid of associated macrophages (Figure 5A). The velocity of the T cells associated with these LVs resembled their average speed in the T zone with *LFA-1*$^{+/+}$ T cells migrating faster than the *LFA-1*$^{-/-}$ T cells (WT, 12.47 ± 0.53 μm/min versus KO, 8.54 ± 0.55 μm/min) (Figure 5B). Towards the periphery of the T zone, the tubular LVs gradually became sparsely associated with auto-fluorescing macrophages (white) (Supplementary Figure 5). The speed of the more peripheral *LFA-1*$^{+/+}$ T cells also decreased to the extent that they now migrated more slowly than the *LFA-1*$^{-/-}$ T cells (WT, 4.45 ± 0.43 μm/min versus KO, 6.48 ± 0.41 μm/min).

In spite of these differences in speed between *LFA-1*$^{+/+}$ and *LFA-1*$^{-/-}$ T cells in the T zone regions, similar proportions contacted and probed the LV membranes (WT, 65.79 ± 5.22% versus KO, 65.23 ± 8.47% (mean ± s.e.m)) (Figure 5C). However, the outcome of this contact was substantially different when the two types of T cells were compared in that a higher proportion of *LFA-1*$^{-/-}$ than *LFA-1*$^{+/+}$ T cells crossed into the LV sinuses (WT,

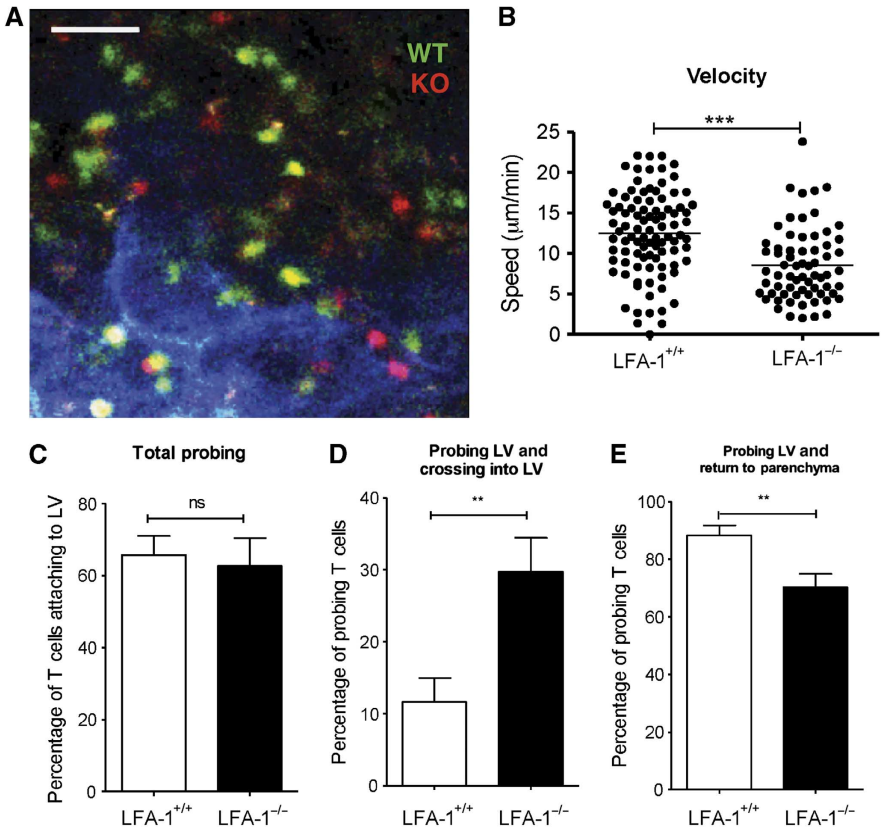

Figure 5 Association of *LFA-1*$^{+/+}$ and *LFA-1*$^{-/-}$ T cells with the lymphatic vessels in the central LV region. (**A**) Intra-vital microscope image of *LFA-1*$^{-/-}$ and *LFA-1*$^{+/+}$ CD4 cells interacting with cortical LV located at 80–150 μm depth from the hilar region where LV (LYVE-1^{+}, blue) appears tubular and macrophage free; scale bar = 50 μm. (**B**) Quantification data for T-cell velocity in areas with x–y axis length of 250 μm encompassing tubular cLV; a total of >150 cells were analysed (WT, 94 cells; KO, 67 cells) combined from 3 experiments. (**C**) Frequency of probing on outer LV walls by both T-cell types. (**D**) Proportion of T cells that crossed into the LV following probing of LV walls. (**E**) Proportion of T cells that returned to T-cell parenchyma following probing behaviour; (**C**–**E**) data combined from $n = 5$ experiments with >400 T cells analysed; T-cell probing and crossing in LV was recorded during an observation time of 30 min.

11.62 ± 3.34% versus KO, 29.73 ± 4.70% (mean ± s.e.m)) (Figure 5D; Supplementary Video 3). Correspondingly, higher numbers of *LFA-1*$^{+/+}$ than *LFA-1*$^{-/-}$ T cells returned to the T-cell parenchyma after making LV contact (WT, 88.37 ± 3.34% versus KO, 70.25 ± 4.71% (mean ± s.e.m)) (Figure 5E).

A question was whether the 2.3-fold decrease in LN dwell time of *LFA-1*$^{-/-}$ compared with *LFA-1*$^{+/+}$ T cells (Figure 1A) could be accounted for by the use of LFA-1 to reverse migrate back into the LN. To investigate this issue, the comparative proportion of *LFA-1*$^{+/+}$ or *LFA-1*$^{-/-}$ T cells leaving the LN at 6 h was determined by calculating the percentage of each T-cell type in contact with LV that subsequently exited over 30 min following adoptive transfer (WT—11.62 × 0.65 = 7.55%; KO—29.73 × 0.65 = 19.32%). Over this time period 2.6-fold more *LFA-1*$^{-/-}$ than *LFA-1*$^{+/+}$ T cells left the LN indicating that their distinctive behaviour at the point of LV contact could account for the effect of LFA-1 on T-cell LN dwell time. This is a rough estimate as it is unknown whether the rate of reverse migration versus exiting is the same at all time points and at all LV contacts within the LN.

In summary, *LFA-1*$^{-/-}$ T cells were able to cross into the LV and did so with almost three times the frequency of *LFA-1*$^{+/+}$ T cells which preferentially reverse migrated back to the node parenchyma following LV contact.

LFA-1$^{+/+}$ *and LFA-1*$^{-/-}$ *T-cell interactions with the distal LV network vessels in the medulla region of the LN*

The final option for exit from the LN is in the medulla although many fewer T cells exited in this region compared with the more centrally located LVs. Immunohistochemical staining showed the medullary LVs to have the appearance of an open meshwork of interconnecting LYVE-1^{+} sinuses (green) intimately associated with numerous MOMA-1^{+} (CD169, sialoadhesin) macrophages (blue) some of which also expressed LYVE-1 (Gordon *et al*, 2010; Figure 6A, *inset*). Both LVs and associated macrophages expressed ICAM-1 (Supplementary Figure 6).

Furthermore, because of the dominance of the meshwork-like LV network in this region it was easier to observe the shape of the T cells, but more difficult to identify individual LV and T-cell entry and exit events. T cells extensively probed the interconnected LV structures by crawling over and adhering to them. *LFA-1*$^{+/+}$ T cells migrated at an average lower velocity than the *LFA-1*$^{-/-}$ T cells (WT, 3.83 ± 0.37 μm/min versus KO, 5.93 ± 0.40 μm/min, $P < 0.001$ (mean ± s.e.m)) (Figure 6B and C; Supplementary Video 4). *LFA-1*$^{+/+}$ T cells frequently appeared elongated, whereas many of the *LFA-1*$^{-/-}$ T cells maintained a rounder morphology. Measurement of the cells' longest versus shortest dimensions indicated that 38.5% of *LFA-1*$^{+/+}$ T cells had axis ratios of

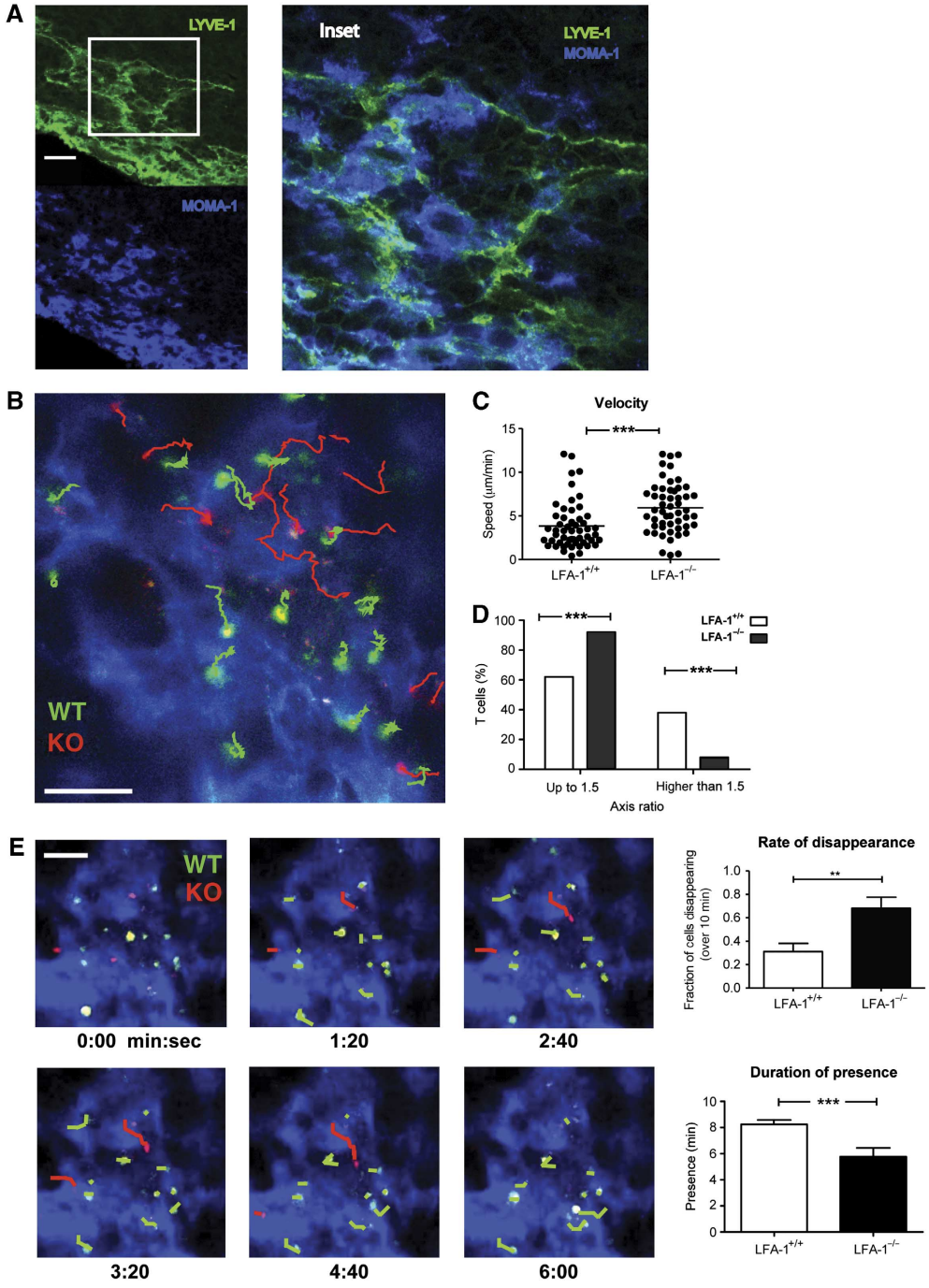

Figure 6 Association of *LFA-1*$^{+/+}$ and *LFA-1*$^{-/-}$ T cells with the LV network in the medulla. (**A**) LYVE-1^{+} LV and MOMA-1/CD169^{+} macrophages in the medulla area. Tissue section of inguinal LN was stained for LYVE-1 (green) and MOMA-1/CD169 (blue) and analysed by confocal microscopy, scale bar = 30 μm; inset shows detail of close association of LV and macrophages; image typical of sections from $n = 3$ LN. (**B**) Migratory behaviour of *LFA-1*$^{+/+}$ (WT, green tracks) and *LFA-1*$^{-/-}$ (KO, red tracks) CD4 T cells on the LYVE-1 network of vessels (blue) viewed from the hilar region at 50 μm depth, scale bar = 50 μm. (**C**) Quantification of velocity is shown for both *LFA-1*$^{+/+}$ and *LFA-1*$^{-/-}$ cells; data combined from two characteristic experiments each with >50 T cells analysed/group. (**D**) Axis ratio of *LFA-1*$^{+/+}$ and *LFA-1*$^{-/-}$ T-cell shape; quantification of the relative proportion of each cell type with a length/width ratio of <1.5 compared with proportion that were >1.5; data combined from three experiments with a total of >100 T cells/type analysed are shown. (**E**) T cells in contact with LYVE-1^{+} LV in the medulla (blue); kinetics of *LFA-1*$^{+/+}$ and *LFA-1*$^{-/-}$ T-cell migration across the LV of the medulla into the efferent lymphatic drainage; paths taken by the T cells over 6 min are indicated (WT: green; KO: red), scale bar = 50 μm; upper right panel: proportion of each T-cell type disappearing into lymphatic drainage and lower right panel: duration of presence or dwell time of each T-cell type during the observation period; data represent the mean ± s.e.m. of two characteristic experiments (45 WT and 25 KO T cells analysed) each observed over a 10-min period.

>1.5 compared with only 7.7% *LFA-1*$^{-/-}$ T cells (Figure 6D). This difference in morphology suggested that the elongated *LFA-1*$^{+/+}$ T cells, unlike the *LFA-1*$^{-/-}$ T cells, were attached and adhesive. Swapping the fluorescent dyes between *LFA-1*$^{+/+}$ and *LFA-1*$^{-/-}$ T cells yielded the same result (Supplementary Figure 7).

Supporting their adhesive appearance, *LFA-1*$^{+/+}$ T cells displayed a more sessile behaviour, while *LFA-1*$^{-/-}$ moved more rapidly over the LV network and disappeared faster from the imaging field. Over a 10-min period, 68% *LFA-1*$^{-/-}$ T cells left the tissue compared with 31% of the *LFA-1*$^{+/+}$ T cells which continued their probing interactions on the LV network (Figure 6E). Correspondingly, the *LFA-1*$^{-/-}$ T cells disappeared quickly with an average lymphatic contact time of 5.7 ± 0.67 min, whereas the *LFA-1*$^{+/+}$ T cells took 8.24 ± 0.33 min to cross the LVs (Figure 6E).

In summary in the medulla the *LFA-1*$^{+/+}$ T cells migrated more slowly than *LFA-1*$^{-/-}$ T cells which correlated with greater adhesive contact with the LV network of cells. In contrast, *LFA-1*$^{-/-}$ T cells were observed to be less adherent and more motile, with the consequence that they exited more rapidly than the *LFA-1*$^{+/+}$ T cells after they had engaged the LV membrane.

An assessment of directionality of T-cell migration at the lymphatic vasculature and its functional implications

As a further measure of the effect of LFA-1 on exiting behaviour, we measured the T-cell migratory angle in association with the LVs in the central paracortical region (Figure 7A). As the LVs were frequently branched and curvaceous, we defined a default exit angle for each individual imaging field according to its planar orientation to the LV and quantified the path length travelled by the T cell within a range of 90° around the specified exit angle. *LFA-1*$^{-/-}$ T cells followed a more direct trajectory compared with *LFA-1*$^{+/+}$ T cells (Figure 7B). This suggested that LFA-1 interactions were dictating the deviation from the most straightforward exit route. The difference disappeared in *ICAM-1*$^{-/-}$ hosts further confirming the role of LFA-1 in the migration pattern at the point of making the exit decision (Figure 7C).

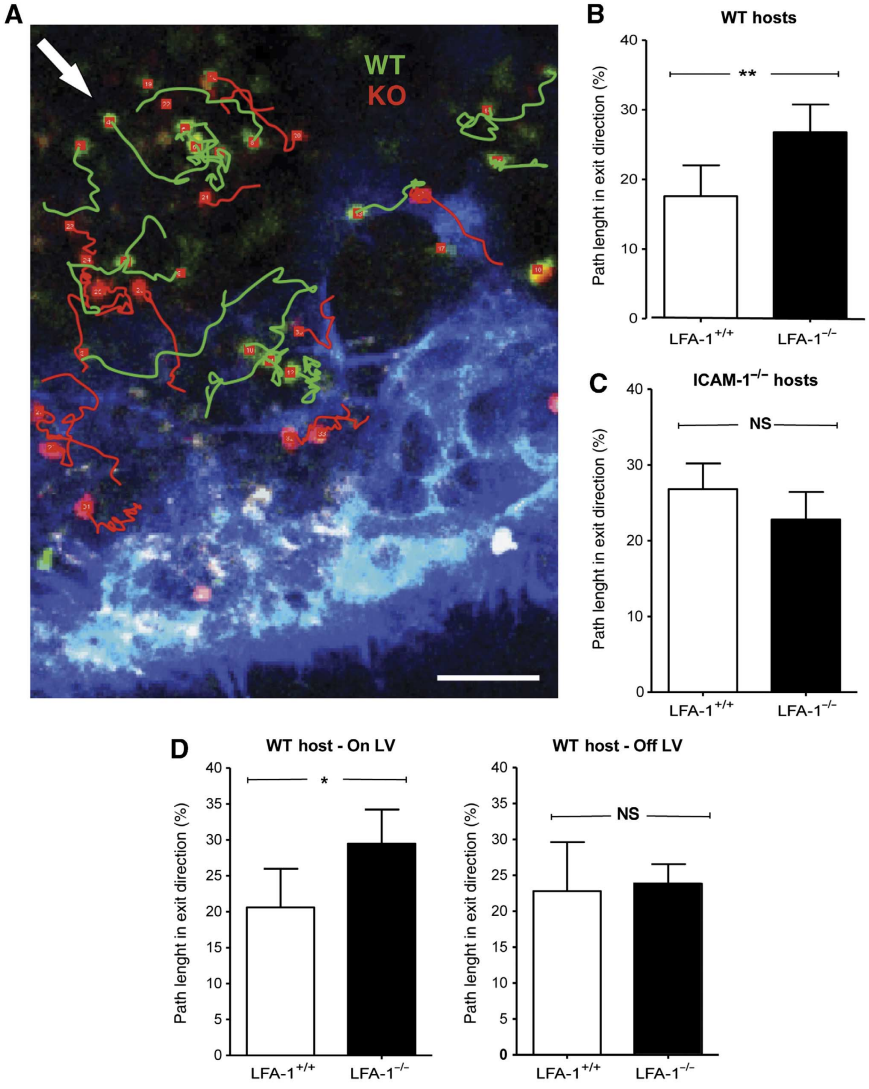

Figure 7 Measurement of directionality of T-cell migration at LV exit structures. (**A**) Migratory behaviour of *LFA-1*$^{+/+}$ and *LFA-1*$^{-/-}$ T cells showing their individual tracks adjacent to LYVE-1+ lymphatic vasculature (blue); exit angle as defined for this field of view indicated by arrow (white); scale bar = 50 μm. (**B**) Quantification of all cumulative path length and orientation data: proportion of *LFA-1*$^{+/+}$ and *LFA-1*$^{-/-}$ T cells in WT hosts migrating in exit direction (within a 90° angle around defined exit angle). (**C**) As (**B**) but in *ICAM-1*$^{-/-}$ hosts. (**D**) A comparison of T cells migrating directly on the LV versus T cells within this area without LV contact during the time of analysis. Data represent the mean of $n = 3$ experiments with >150 cells total analysed in each experimental group during an observation time of 30 min.

To test whether the direction of migration was influenced by the LV directly or alternatively by closely associated cells in the immediate microenvironment, we looked at directionality of T cells both on and off the LV. *LFA-1*$^{+/+}$ T cells displayed a more random directionality compared with *LFA-1*$^{-/-}$ T cells when in direct contact with LV, whereas their migratory behaviour did not differ when not in contact (Figure 7D). Thus, the more random migration of *LFA-1*$^{+/+}$ T cells at the point of LV exit is dictated by direct contact with LV.

A role for ICAM-1-expressing LV in increased immune responsiveness

It was important to clarify whether prolonged T-cell contact with ICAM-1-expressing LVs might be an epi-phenomenon without biological significance or would directly affect T-cell function. A reasonable hypothesis was that such contact aiding reverse migration back into the LN would allow T cells further opportunities to encounter any antigen-laden APC thus enhancing an immune response. To discriminate between the use of LFA-1/ICAM-1 for optimal antigen presentation and LV egress behaviour, we adoptively transferred equal numbers of WT DCs pre-incubated or not with ovalbumin peptide (pOVA) into the footpads of *ICAM-1*$^{-/-}$ and WT hosts as previously described (Mempel *et al*, 2004; Lammermann *et al*, 2008). CFSE-labelled OVA-TCR transgenic OT-2 CD4 T cells were injected i.v. 16 h later. Previous studies have shown overlapping roles for ICAM-1 and ICAM-2 in LN homing, suggesting that OT-2 T cells would not be significantly delayed in entry into the LN of *ICAM-1*$^{-/-}$ host mice (Lehmann *et al*, 2003; Boscacci *et al*, 2010) and we observed this to be the case (WT, 3315 ± 843 versus KO, 2270 ± 551 homing OT-2 T cells; $n = 3$ experiments). In this context, the OT-2 T cells should have an equivalent opportunity for stimulation in each host. When proliferation of the T cells isolated from ipsilateral LNs was assessed at 72 h, proliferation in the nodes of *ICAM-1*$^{-/-}$ hosts was significantly reduced compared with WT hosts (Figure 8A and B). There was also a trend for ongoing proliferation in the contralateral LN of the WT host, suggesting that stimulated T cells had already left the directly stimulated LN. These experiments indicate that LFA-1 contributes to an immune response not only via the well-described interaction between T cells and DCs but also at the level of the LVs.

Discussion

It is well established that T-cell migration across the high endothelial vasculature into LN relies on the integrin LFA-1 (Hamann *et al*, 1988; Berlin-Rufenach *et al*, 1999). In this study, we have asked whether LFA-1 plays any role within the LN during the trafficking of T cells that continually circulate between blood and the LNs. We found that *LFA-1*$^{-/-}$ CD4 T cells spend less time in the LN than *LFA-1*$^{+/+}$ lymphocytes yet show similar behaviour in *ICAM-1*$^{-/-}$ host mice. Intravital microscopy revealed that after probing the surface of LVs, *LFA-1*$^{+/+}$ T cells more frequently returned back into the LN, whereas *LFA-1*$^{-/-}$ T cells had a greater tendency to exit. Thus, T cells did not require LFA-1 to exit, but rather LFA-1-mediated adhesion to the LV contributed to reverse migration back into the LN parenchyma.

We first verified that the reduced dwell time of *LFA-1*$^{-/-}$ T cells in the LN was not accounted for by lack of niche access nor speed of migration within the T zone. In fact, *LFA-1*$^{-/-}$ T cells migrated somewhat more slowly than *LFA-1*$^{+/+}$ T cells, a deficit also observed in *CD18*$^{-/-}$ T cells (Woolf *et al*, 2007). This difference was lost in host mice lacking the LFA-1 ligand ICAM-1. Comparison of the migration in different areas of the LN revealed a gradual decrease in T cell speed from central T zone to the peripheral and medullary regions, that predominantly affected *LFA-1*$^{+/+}$ T cells. The slower speed in the medulla has previously also been noted by others (Wei *et al*, 2005; Sanna *et al*, 2006; Nombela-Arrieta *et al*, 2007; Grigorova *et al*, 2009, 2010).

The speed of T-cell migration may be influenced by locally regulated LFA-1 activation and deactivation brought about through contacts in the densely cellular LN microenvironment where ICAM-1 varies. A feature of DC migration, for example, is chemokine-induced adhesion to ICAM-1-expressing stromal cells (Schumann *et al*, 2010). However, the use of knock-in T cells expressing LFA-1 in a primed intermediate affinity conformation suggests that regulated LFA-1 activity is not involved in motility within the LN parenchyma (Park *et al*, 2010). It is currently difficult to reconcile these conflicting data.

However, the varying speeds of migration within the T zone do not provide an explanation for a faster exit rate of *LFA*$^{-/-}$ T cells from the LN. A clue to this different behaviour was the finding that *LFA-1*$^{+/+}$ CD4 T cells had increased presence over *LFA-1*$^{-/-}$ cells in regions of the LN where LVs were most concentrated. A key finding was that the *LFA-1*$^{+/+}$ T cells reverse migrated back into the LN more frequently than *LFA-1*$^{-/-}$ T cells after probing the LV walls. An observation was that the paths of the *LFA-1*$^{-/-}$ T cells on the LV were straighter than those of the *LFA-1*$^{+/+}$ T cells which displayed more random trajectories correlating with frequency of in migration back into the node parenchyma. As this LFA-1-mediated activity took place on the LV walls, it was relevant to demonstrate that the ligand ICAM-1 was expressed by the non-stimulated LV for which there has previously been both positive and negative evidence (Johnson *et al*, 2006; Link *et al*, 2007). In addition, the differences in the T-cell trajectories disappeared in *ICAM-1*$^{-/-}$ host mice.

The arrival of T cells at the point of egress occurs stochastically as a balance of responsiveness to retaining factors such as CCL21 and factors influencing egress such as S1P. Our study indicates that adhesion through LFA-1 is another factor determining egress potential. In *in vitro* chemotaxis assays, the state of LFA-1 expression had no impact on the response to CCL21 and S1P whether the assays were ICAM-1 dependent or independent. In seeming conflict is our data indicating that the LFA-1/ICAM-1 interaction dictates how T cells migrate on the LV. The requirement for shear flow conditions to activate LFA-1 on recirculating primary T cells has been reported by Woolf *et al* (2007) and we show that *LFA-1*$^{+/+}$ CD4 T cells, but not *LFA-1*$^{-/-}$ T cells, adhered and migrated under shear flow conditions on ICAM-1 in response to both immobilised S1P and CCL21. The LVs display fluid flow, but the parenchyma of the LN is considered to be shear free at least in terms of fluid. We show that T cells are adhering in an LFA-1-dependent way on the LV but not in the adjacent areas. One explanation is that the expression or organisation of ICAM-1 on LV surface activates LFA-1. Alternatively, T cells

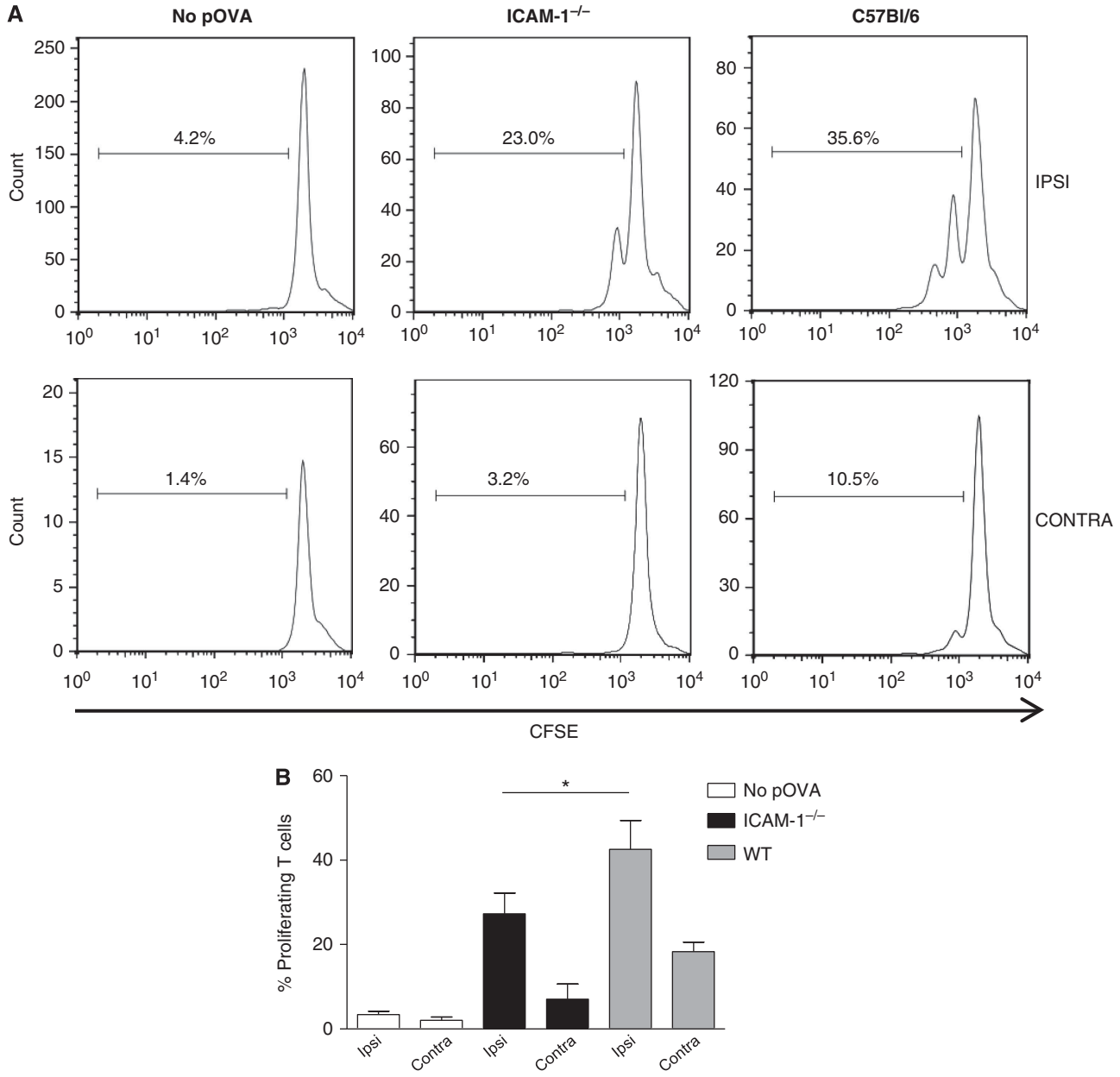

Figure 8 Response of OT-2 transgenic T cells in WT and ICAM-1 host mice. (**A**) The proportion of proliferating CFSE-labelled OT-2 T cells exposed to WT dendritic cells pre-incubated or not with pOVA in either WT or *ICAM-1*$^{-/-}$ host mice; dendritic cells were injected into hind foot pad and both ipsilateral (IPSI) and contralateral (CONTRA) lymph nodes were examined at 72 h following i.v. injection of OT-2 CD4 T cells; (**B**) combined data from $n = 3$ experiments showing the extent of proliferation in both ipsilateral and contralateral nodes as in (**A**).

interacting with HEV bear filipodia expressing LFA-1 that extend into the HEV from the leading edge (Shulman *et al*, 2009; Heasman *et al*, 2010). This might provide another possible means of LFA-1 activation if a similar process occurs when T cells interact with LVs.

These data are consistent with reports that the interaction of S1P1 with its ligand S1P causes integrin activation (Paik *et al*, 2001; Ledgerwood *et al*, 2008) and that *S1P1*$^{-/-}$ T cells are deficient in firm adhesion to LN HEVs under flow conditions, an LN entry step that is integrin mediated (Halin *et al*, 2005). In terms of distribution, S1P is LV associated as well as being present in lymph and therefore in position to influence LFA-1 activity on the T cells (Pham *et al*, 2008; Grigorova *et al*, 2009). Although the initial lymphatics express CCL21 (Tal *et al*, 2011), it is not yet established whether chemokines within the LN are LV tethered (Randolph *et al*, 2005). Thus, it is tempting to speculate that local concentration of LV-associated S1P might be responsible for stimulating the random migratory trajectory of *LFA-1*$^{+/+}$ T cells at the LV membrane via its LFA-1 activating function.

Our study provides evidence that LFA-1-mediated migration on the LV contributes to the balance of factors determining whether or not a T cell will leave the LN. A key issue is what T-cell functions might be influenced by this behaviour. Contact of DCs with LVs can suppress their activation, suggesting a role for lymphatic membranes in influencing the state of leukocyte activation (Podgrabinska *et al*, 2009).

However, revisiting of the T zone parenchyma gives T cells further opportunity to scan for antigen-loaded presenting cells and to subsequently become activated. This might be a particularly decisive mechanism for effective immune activation when the numbers of cognate APC in an LN or the amount of presented antigen on their surface are low. We provide evidence that such a mechanism does indeed function *in vivo*. Stimulation of OT-2 transgenic T cells by ovalbumin-laden ICAM-1-expressing DCs in a WT host was 30% more efficient compared with the same situation in an *ICAM-1*$^{-/-}$ host. Collectively, these data show that intranodal T-cell activation is not only dependent on the LFA-1-ICAM-1 axis during T-cell/APC interaction, but also during migration on and contact formation with LVs.

Our data add to previous reports that T cells engage in one or more rounds of shuttling between T zone parenchyma and the LV prior to finally exiting (Grigorova *et al*, 2009, 2010). LFA-1-mediated adhesion contributes to this reverse migration back into the node parenchyma. We propose that this behaviour increases the probability on a per T-cell basis of encountering APC-associated antigen. In contrast, according to the concept of immune surveillance, T cells enhance their opportunities of encountering foreign antigen by recirculating around the body and entering into and exiting from many LNs. However, this LFA-1-mediated shuttling of T cells may make an additional contribution to immune surveillance at the level of the individual LN.

In terms of LN entry across the HEV, LFA-1 supplies adhesive support for the T cells enabling them to withstand the force of blood flow and to migrate across the HEV into the node. Conversely, at the point of leaving the LN, LFA-1-mediated T cell contacts with LV membranes represent a critical contribution in shaping whether or not T cells exit. Thus, LFA-1 contributes to the functions that T cells perform both at the beginning and end of their LN journey.

Materials and methods

Mice

LFA-1$^{-/-}$ mice were bred on the C57BL/6JCrl to backcross generation 12 (Berlin-Rufenach *et al*, 1999). *ICAM-1*$^{-/-}$ mice (C57BL/6J) were obtained from Drs Britta Engelhardt and Urban Deutsch (Theodor Kocher Institute, Bern, Switzerland) with the permission of Dr Arthur Beaudet (Baylor College, Houston, TX, USA) (Bullard *et al*, 2007). Sex-matched 5- to 12-week-old mice were used in the experiments. Mice transgenic for 3A9 TCR specific for I-A^{k}/HEL$^{46\text{-}71}$ were on a B10.BR background (Jackson Laboratory, Bar Harbor, ME, USA) and bred at LRI (Ho *et al*, 1994). All animal experiments were approved by the Landesverwaltungsamt Sachsen-Anhalt (file number: 203.h-42502-2-874 Uni MD) and the United Kingdom Home Office.

Purification of CD4+ T lymphocytes

CD4 splenic and LN T cells were enriched by negative isolation via immunomagnetic depletion using a mouse CD4+ T cell Isolation kit (MACS Miltenyi Biotech) with purity of >95% as assessed by flow cytometry. In some experiments, naïve CD4 T cells were isolated by FACS through gating on the CD4 T cells and sorting the CD44^{lo} cell population.

Flow cytometry

Leukocytes (5×10^5) were incubated on ice in 50 μl of PBS/0.1% BSA containing the following directly conjugated mAbs at optimal dilution: CD4-APC or -FITC (RM4-5, eBioscience or BD Biosciences); CD44-FITC or -BrilliantViolet421 (IM7, PharMingen or Biolegend); CD62L-APC-eFluor780 (MEL-14, eBioscience); CD69-PE (eBioscience). In some experiments, intact LNs were cultured under appropriate conditions, then fluorochrome-labelled CD4 T cells were tested for state of apoptosis using biotinylated Annexin V (Invitrogen) detected with Streptavidin-Pacific Blue.

Immunoblotting

Cell lysates, prepared as previously described (Svensson *et al*, 2009), were separated using pre-cast 3–8% SDS–PAGE gels (Invitrogen) and transferred onto PVDF membrane (Immobilon-P, Millipore). Blots were probed with rabbit anti-S1P1 (EDG-1, H-60, Santa Cruz), rat CCR7 mAb (4B12, eBioscience) and mouse anti-α-tubulin mAb (Sigma Aldrich Ltd), followed by secondary Abs: goat anti-rabbit Ig-HRP, rabbit anti-rat Ig-HRP, and sheep anti-mouse Ig-HRP (all Dako Ltd) and ECL detection reagents (GE Healthcare).

Chemotaxis

Splenocytes were washed twice in 0.1% fatty acid-free BSA (Sigma Aldrich Ltd) and incubated for 1 h at 37°C prior to incubation at 1×10^6 cells/100 μl in 5 μm pore Transwell insert wells (Corning) that were either uncoated or coated overnight with mouse ICAM-1-Fc at 1 μg/ml. The lower wells contained either 600 μl RPMI-1640/0.1% fatty acid-free BSA, medium plus 25 nM S1P (Biomol/Enzo Life Sciences) or 6 μM CXCL21 (PeproTech EC Ltd) with dose level determined by titration. After incubation at 37°C for 2.5 h on uncoated filters or the shorter time of 1.5 h on ICAM-1-coated wells (to detect rapid migration), the chambers were rested on ice for 20 min, inserts discarded and the migrated cells recovered using ice-cold 5 mM EDTA/PBS. CD4 T cells were identified by flow cytometry and enumerated with the aid of counting beads (CountBright absolute counting beads, Invitrogen).

Shear flow assay

ibiTreat μ-slide VI flow chambers (Ibidi) were coated overnight with protein A (0.5 mg/ml, Sigma-Aldrich Ltd), then incubated with 2% fatty acid-free BSA for 30 min at RT followed by mouse ICAM-1Fc (1 μg/ml), S1P (1 μM), or CCL21 (6 μM). Purified CD4 T cells (5×10^5 cells/ml) were allowed to attach for 15 min at 37°C in 20 mM HEPES pH 7 in HBSS, then flow conditions of 1 dyn cm^2 were implemented using an automated syringe pump (KDS model 200; Linton Instrumentation) as previously reported (Evans *et al*, 2011). The adhesion/migration characteristics of T cells were recorded using a 20× lens on a Nikon Diaphot 300 microscope, a Sony XCD-X700 camera and AQM^{2001} Kinetic Acquisition Manager software (Kinetic Imaging Ltd, Bromborough, UK). Images were taken every 2 s for 3 min.

Immunofluorescence: in vitro and in vivo labelling

For immunohistology, snap-frozen inguinal LNs were cut in 10 μm sections, fixed in 4% paraformaldehyde, blocked in 1% BSA and 10% rabbit serum and stained for 1 h at RT with various mAbs and pAbs: FITC-CD3, PE-B220 (eBioscience); ICAM-1-Biotin (YN1/1.7.4, eBioscience). Biotinylated primary mAbs were detected using Streptavidin-AlexaFluor555 (Invitrogen). LYVE-1 (clone 223322, R&D Systems, Europe) was directly labelled with AlexaFluor488, AlexaFluor546 or Pacific Blue (Molecular Probes) and MOMA-1 (CD169, Bachem or Acris) was directly labelled with AlexaFluor680 or Pacific blue. Sections were assessed using LSM 510 and 710 confocal microscopes using 20×/0.8 Plan-Apochromat and 40×/1.3 Plan-NEOFLUAR DIC oil objectives and capturing images using, respectively, LSM 510 software and Software Zen 2009 (Zeiss).

Pixel-by-pixel determination of overlap between ICAM-1 and LYVE-1 staining was analysed using ImageJ software. Each fluorescence channel was treated separately by giving a value of 1.0 to each pixel to indicate positive staining and then the two values derived from ICAM-1 and LYVE-1 staining were multiplied. Staining of LYVE-1 was set at 100% to obtain percentages for co-staining with ICAM-1.

Adoptive transfer of T cells for homing and intra-vital studies

For adoptive transfer studies, CD4 T cells from *LFA-1*$^{-/-}$ and *LFA-1*$^{+/+}$ control C57BL/6JCrl mice at 5×10^6 cells/ml in 5% FCS/RPMI were labelled as described (Berlin-Rufenach *et al*, 1999). Briefly, T cells were incubated with either 0.5 μM CFSE or 5 μM SNARF-1 (all Molecular Probes) according to manufacturer's protocol at 37°C for 45 min. The differentially labelled T-cell preparations were mixed at 5×10^6 cells each to achieve a 1:1 ratio of *LFA-1*$^{+/+}$ and

LFA-1$^{-/-}$ cells for i.v. injection into recipient mice. For quantification of the entry ratio, a correction factor was applied to the subsequent data if the injected lymphocyte ratio was not 1:1.

To block further lymphocyte entry, 100 μg each of purified rat mAbs MEL 14 (L-selectin, CD62L) and PS2/3 (α4, CD47d) per mouse were injected i.v. at 6 h post T-cell transfer. To test the efficiency of this blockade while simultaneously mimicking the LN trafficking experiments, endotoxin-free L-selectin mAb MEL-14 and α4 integrin mAb PS2/3 or PBS as a control were injected 30 min prior to the fluorochrome-labelled T cells (5×10^6 per cell type), then LN T-cell numbers were assessed 4 h later (see text). PS2/3 was prepared by the CR UK Monoclonal Antibody Service; MEL-14 was a kind gift of Dr Alf Hamann, Charite Universitaetsmedizin Berlin, Germany and purchased from eBioscience.

For two-photon imaging, T cells were stained with 5 μm CFSE, 5 μM Cell Tracker Orange (CTO) or 5 μM Cell Tracker Blue (CTB) (all from Molecular Probes) according to manufacturer's protocols and as previously described (Reichardt *et al*, 2007b). Colours were routinely swapped between experiments. For *in vivo* labelling of LV, anti-mouse LYVE-1 labelled with Alexa 546 or Pacific Blue at 5–10 μg in 30 μl PBS was injected s.c. in the mouse flank 24 h before imaging. To visualise dynamics of lymph flow, FITC dextran (2 MDa, Sigma-Aldrich Ltd) was applied s.c. into the right footpad at 2 h and 30 min before imaging.

Two-photon microscopy

Fluorescently labelled, purified CD4 T cells (1:1 ratio, 5×10^6 per cell type) were injected i.v. into the tail vein of 5- to 6-week-old C57BL/6 mice at 6 h before imaging as previously described (Gunzer *et al*, 2004; Reichardt *et al*, 2007a, b). For some experiments, the KO:WT ratio was increased up to 5:1 cells to compensate for the deficiency of LN entry of *LFA-1*$^{-/-}$ T cells. The ratio or time of natural homing, without the use of blocking antibodies, in the time window chosen had no effect on viability or motility behaviour of the T cells imaged.

For intra-vital microscopy, anaesthesia of mice was initiated with i.p. application of 30 mg/kg ketamine (Inresa, Freiburg, Germany) plus 3 mg/kg xylazine (Bayer Health Care, Leverkusen, Germany) followed by intra-tracheal intubation and ventilation with oxygen-isoflurane (Deltaselect, Pfullingen, Germany). The inguinal LN was exposed by surgically removing surrounding tissue carefully sparing blood and lymph vessels. Quality of regional perfusion and oxygenation under anaesthesia was monitored oxymetrically (O2C, LEA, Giessen, Germany), and temperature maintained at 37°C. For *ex vivo* imaging of explanted LN, organs were kept in PBS and imaged immediately after being explanted. Single scan fields of typically 303 × 303 μm were imaged, which in some experiments were tiled to combine up to 3636 × 3636 μm combined fields.

Two-photon microscopy was performed using a ZeissLSM710 microscope (Carl Zeiss, Jena, Germany) equipped with a MaiTai DeepSee Femtosecond-Laser (Spectra-Physics, Darmstadt, Germany) typically tuned to 800 nm on an AxioExaminer upright stage with a 20×, NA 1.0 (Zeiss) water dipping lens. Image detection was done with three non-descanned (NDD) detectors typically equipped with emission detection filters of 565–610 nm (red), 500–500 (green), and ShortPass485 (blue). Individual RGB z-stacks of max 606 × 606 μm images were recorded in single plane or multiple z-planes as indicated, for time-lapse sequences typically every 4–20 s and lasting typically 15–30 min. Image rendering was performed using Volocity 4.3 (Improvision, Waltham, MA, USA). Cell tracking was done using the ImageJ Plugin ManualTracker and the computer-assisted manual tracking software CellTracker as described before (Reichardt *et al*, 2007b).

CellTracker software was also used for computing path length within exit angles. For each path of movement of individual cells as recorded by the software between two observation points, a directional xy angle was automatically assigned. This allowed quantification of the summary path lengths in each directional angle for each T-cell population. When comparing with the exit angle defined for the field of view based on its positioning in the LN, the percentage of path length in exit direction (exit angle ±90°) could be quantified and allowed a measure of the propensity to exit for this cell type. Data were plotted with Prism 4 (GraphPad Software, San Diego, CA, USA).

Adoptive transfer of dendritic and T cells for testing immune responsiveness

DCs were prepared as previously reported (Gunzer *et al*, 2000; Reichardt *et al*, 2007a). Briefly, bone marrow-derived cells (BMDCs) were differentiated in RPMI-based media with IL-4 and GM-CSF for 7 days and treated with 20 ng/ml LPS (*E. coli* 0111, B4; Sigma, Deisenhofen, Germany) on day 7. On day 8, OVA peptide (pOVA, AS 323-339 from chicken ovalbumin, Peptide Core facility, HZI, Braunschweig, Germany) was added at 20 ng/ml to the culture. After 4 h of co-incubation with pOVA, non-adherent DC was harvested, extensively washed to remove excess peptide and injected (0.5×10^6 in 20 μl PBS) into the right hind footpad of age-matched C57/BL6 WT or *ICAM-1*$^{-/-}$ hosts as in Mempel *et al* (2004) and Lammermann *et al* (2008). As a control, DC from the same culture (but not peptide loaded) was injected into the right hind footpad of WT hosts. After 16 h, CD4 T cells from OVA TCR-transgenic OT-2 mice (Barnden *et al*, 1998) were obtained by negative isolation. All OT-2 cells were stained with 10 μM CFSE as described (Reichardt *et al*, 2007a) and 5×10^6 cells were injected retro-orbitally into each host. Seventy-two hours later ipsilateral and contralateral popliteal nodes were prepared separately and the contained leukocytes were labelled with fluorochrome-conjugated antibodies against CD4 and analysed for proliferation by CFSE dilution using flow cytometry on a MCAS-Quant system (Miltenyi, Bergisch-Gladbach, Germany).

Statistical analysis

The statistical package within GraphPad Prism 4 was used for analysing data. Student's *t*-test or a non-parametric test (Mann–Whitney) or Fisher's Exact Test (for analysis of a contingency table) was applied to assess statistical significance. Significance levels employed are indicated in Results; **P*-value <0.05; ***P*-value <0.01; ****P*-value <0.001 were considered as significant.

Supplementary data

Supplementary data are available at *The EMBO Journal* Online (http://www.embojournal.org).

Acknowledgements

We are most grateful for the help of CRUK colleagues Emma Nye, Experimental Pathology for immunohistochemistry technology; Stuart Horswell, Bioinformatics and Biostatistics; Andy Filby, FACS Laboratory; Frederic Bollet-Quivogne, Light Microscopy; Katie Bentley, Vascular Biology for computational help; Neil Rogers and Caetano Reis e Sousa for transgenic mice. We also thank Alf Hamann, Berlin for generous supplies of mAb MEL-14. This work was supported by Cancer Research UK (NH and IP), C. J. Martin Fellowship (KJ) and by the German Research Foundation through grant SFB854 (PR and MG) and SPP1468 (to MG).

Author contributions: IP, PR, EE and KJ performed the experiments, compiled data and commented on the manuscript, MG supervised intra-vital technology, T cell proliferation experiments and helped with the manuscript, NH directed the project and wrote the manuscript.

Conflict of interest

The authors declare that they have no conflict of interest.

References

Bajenoff M, Egen JG, Koo LY, Laugier JP, Brau F, Glaichenhaus N, Germain RN (2006) Stromal cell networks regulate lymphocyte entry, migration, and territoriality in lymph nodes. *Immunity* **25:** 989–1001

Bajenoff M, Egen JG, Qi H, Huang AY, Castellino F, Germain RN (2007) Highways, byways and breadcrumbs: directing lymphocyte traffic in the lymph node. *Trends Immunol* **28:** 346–352

Barnden MJ, Allison J, Heath WR, Carbone FR (1998) Defective TCR expression in transgenic mice constructed using cDNA-based alpha- and beta-chain genes under the control of heterologous regulatory elements. *Immunol Cell Biol* **76:** 34–40

Berlin-Rufenach C, Otto F, Mathies M, Westermann J, Owen MJ, Hamann A, Hogg N (1999) Lymphocyte migration in lymphocyte function-associated antigen (LFA)-1-deficient mice. *J Exp Med* **189:** 1467–1478

Boscacci RT, Pfeiffer F, Gollmer K, Sevilla AI, Martin AM, Soriano SF, Natale D, Henrickson S, von Andrian UH, Fukui Y, Mellado M, Deutsch U, Engelhardt B, Stein JV (2010) Comprehensive analysis of lymph node stroma-expressed Ig superfamily members reveals redundant and nonredundant roles for ICAM-1, ICAM-2, and VCAM-1 in lymphocyte homing. *Blood* **116:** 915–925

Bullard DC, Hu X, Schoeb TR, Collins RG, Beaudet AL, Barnum SR (2007) Intercellular adhesion molecule-1 expression is required on multiple cell types for the development of experimental autoimmune encephalomyelitis. *J Immunol* **178:** 851–857

Carrasco YR, Fleire SJ, Cameron T, Dustin ML, Batista FD (2004) LFA-1/ICAM-1 interaction lowers the threshold of B cell activation by facilitating B cell adhesion and synapse formation. *Immunity* **20:** 589–599

Evans R, Lellouch AC, Svensson L, McDowall A, Hogg N (2011) The integrin LFA-1 signals through ZAP-70 to regulate expression of high affinity LFA-1 on T lymphocytes. *Blood* **117:** 3331–3342

Evans R, Patzak I, Svensson L, De Filippo K, Jones K, McDowall A, Hogg N (2009) Integrins in immunity. *J Cell Sci* **122:** 215–225

Girard JP, Moussion C, Forster R (2012) HEVs, lymphatics and homeostatic immune cell trafficking in lymph nodes. *Nat Rev Immunol* **12:** 762–773

Gordon EJ, Rao S, Pollard JW, Nutt SL, Lang RA, Harvey NL (2010) Macrophages define dermal lymphatic vessel calibre during development by regulating lymphatic endothelial cell proliferation. *Development* **137:** 3899–3910

Gowans JL (1957) The effect of the continuous re-infusion of lymph and lymphocytes on the output of lymphocytes from the thoracic duct of unanaesthetized rats. *Br J Exp Pathol* **38:** 67–78

Grakoui A, Bromley SK, Sumen C, Davis MM, Shaw AS, Allen PM, Dustin ML (1999) The immunological synapse: a molecular machine controlling T cell activation. *Science* **285:** 221–227

Gretz JE, Norbury CC, Anderson AO, Proudfoot AE, Shaw S (2000) Lymph-borne chemokines and other low molecular weight molecules reach high endothelial venules via specialized conduits while a functional barrier limits access to the lymphocyte microenvironments in lymph node cortex. *J Exp Med* **192:** 1425–1440

Grigorova IL, Panteleev M, Cyster JG (2010) Lymph node cortical sinus organization and relationship to lymphocyte egress dynamics and antigen exposure. *Proc Natl Acad Sci USA* **107:** 20447–20452

Grigorova IL, Schwab SR, Phan TG, Pham TH, Okada T, Cyster JG (2009) Cortical sinus probing, S1P1-dependent entry and flow-based capture of egressing T cells. *Nat Immunol* **10:** 58–65

Gunzer M, Schafer A, Borgmann S, Grabbe S, Zanker KS, Brocker EB, Kampgen E, Friedl P (2000) Antigen presentation in extracellular matrix: interactions of T cells with dendritic cells are dynamic, short lived, and sequential. *Immunity* **13:** 323–332

Gunzer M, Weishaupt C, Hillmer A, Basoglu Y, Friedl P, Dittmar KE, Kolanus W, Varga G, Grabbe S (2004) A spectrum of biophysical interaction modes between T cells and different antigen-presenting cells during priming in 3-D collagen and *in vivo*. *Blood* **104:** 2801–2809

Halin C, Scimone ML, Bonasio R, Gauguet JM, Mempel TR, Quackenbush E, Proia RL, Mandala S, von Andrian UH (2005) The S1P-analog FTY720 differentially modulates T-cell homing via HEV: T-cell-expressed S1P1 amplifies integrin activation in peripheral lymph nodes but not in Peyer patches. *Blood* **106:** 1314–1322

Hamann A, Jablonski-Westrich D, Duijvestijn A, Butcher EC, Baisch H, Harder R, Thiele HG (1988) Evidence for an accessory role of LFA-1 in lymphocyte-high endothelium interaction during homing. *J Immunol* **140:** 693–699

Heasman SJ, Carlin LM, Cox S, Ng T, Ridley AJ (2010) Coordinated RhoA signaling at the leading edge and uropod is required for T cell transendothelial migration. *J Cell Biol* **190:** 553–563

Ho WY, Cooke MP, Goodnow CC, Davis MM (1994) Resting and anergic B cells are defective in CD28-dependent costimulation of naive CD4+ T cells. *J Exp Med* **179:** 1539–1549

Johnson LA, Clasper S, Holt AP, Lalor PF, Baban D, Jackson DG (2006) An inflammation-induced mechanism for leukocyte transmigration across lymphatic vessel endothelium. *J Exp Med* **203:** 2763–2777

Katakai T, Hara T, Sugai M, Gonda H, Shimizu A (2004) Lymph node fibroblastic reticular cells construct the stromal reticulum via contact with lymphocytes. *J Exp Med* **200:** 783–795

Klinger A, Gebert A, Bieber K, Kalies K, Ager A, Bell EB, Westermann J (2009) Cyclical expression of L-selectin (CD62L) by recirculating T cells. *Int immunol* **21:** 443–455

Lammermann T, Bader BL, Monkley SJ, Worbs T, Wedlich-Soldner R, Hirsch K, Keller M, Forster R, Critchley DR, Fassler R, Sixt M (2008) Rapid leukocyte migration by integrin-independent flowing and squeezing. *Nature* **453:** 51–55

Ledgerwood LG, Lal G, Zhang N, Garin A, Esses SJ, Ginhoux F, Merad M, Peche H, Lira SA, Ding Y, Yang Y, He X, Schuchman EH, Allende ML, Ochando JC, Bromberg JS (2008) The sphingosine 1-phosphate receptor 1 causes tissue retention by inhibiting the entry of peripheral tissue T lymphocytes into afferent lymphatics. *Nat Immunol* **9:** 42–53

Lehmann JC, Jablonski-Westrich D, Haubold U, Gutierrez-Ramos JC, Springer T, Hamann A (2003) Overlapping and selective roles of endothelial intercellular adhesion molecule-1 (ICAM-1) and ICAM-2 in lymphocyte trafficking. *J Immunol* **171:** 2588–2593

Link A, Vogt TK, Favre S, Britschgi MR, Acha-Orbea H, Hinz B, Cyster JG, Luther SA (2007) Fibroblastic reticular cells in lymph nodes regulate the homeostasis of naive T cells. *Nat Immunol* **8:** 1255–1265

Lo CG, Xu Y, Proia RL, Cyster JG (2005) Cyclical modulation of sphingosine-1-phosphate receptor 1 surface expression during lymphocyte recirculation and relationship to lymphoid organ transit. *J Exp Med* **201:** 291–301

Matheu MP, Cahalan MD, Parker I (2011) Immunoimaging: studying immune system dynamics using two-photon microscopy. *Cold Spring Harb Protoc* **2011:** 147–155

Mempel TR, Henrickson SE, Von Andrian UH (2004) T-cell priming by dendritic cells in lymph nodes occurs in three distinct phases. *Nature* **427:** 154–159

Miller MJ, Wei SH, Parker I, Cahalan MD (2002) Two-photon imaging of lymphocyte motility and antigen response in intact lymph node. *Science* **296:** 1869–1873

Nombela-Arrieta C, Mempel TR, Soriano SF, Mazo I, Wymann MP, Hirsch E, Martinez AC, Fukui Y, von Andrian UH, Stein JV (2007) A central role for DOCK2 during interstitial lymphocyte motility and sphingosine-1-phosphate-mediated egress. *J Exp Med* **204:** 497–510

Paik JH, Chae S, Lee MJ, Thangada S, Hla T (2001) Sphingosine 1-phosphate-induced endothelial cell migration requires the expression of EDG-1 and EDG-3 receptors and Rho-dependent activation of alpha vbeta3- and beta1-containing integrins. *J Biol Chem* **276:** 11830–11837

Park EJ, Peixoto A, Imai Y, Goodarzi A, Cheng G, Carman CV, von Andrian UH, Shimaoka M (2010) Distinct roles for LFA-1 affinity regulation during T-cell adhesion, diapedesis, and interstitial migration in lymph nodes. *Blood* **115:** 1572–1581

Pham TH, Okada T, Matloubian M, Lo CG, Cyster JG (2008) S1P1 receptor signaling overrides retention mediated by G alpha i-coupled receptors to promote T cell egress. *Immunity* **28:** 122–133

Podgrabinska S, Kamalu O, Mayer L, Shimaoka M, Snoeck H, Randolph GJ, Skobe M (2009) Inflamed lymphatic endothelium suppresses dendritic cell maturation and function via Mac-1/ICAM-1-dependent mechanism. *J Immunol* **183:** 1767–1779

Randolph GJ, Angeli V, Swartz MA (2005) Dendritic-cell trafficking to lymph nodes through lymphatic vessels. *Nat Rev Immunol* **5:** 617–628

Reichardt P, Dornbach B, Rong S, Beissert S, Gueler F, Loser K, Gunzer M (2007a) Naive B cells generate regulatory T cells in the presence of a mature immunologic synapse. *Blood* **110:** 1519–1529

Reichardt P, Gunzer F, Gunzer M (2007b) Analyzing the physicodynamics of immune cells in a three-dimensional collagen matrix. *Methods Mol Biol* **380:** 253–269

Sanna MG, Wang SK, Gonzalez-Cabrera PJ, Don A, Marsolais D, Matheu MP, Wei SH, Parker I, Jo E, Cheng WC, Cahalan MD, Wong CH, Rosen H (2006) Enhancement of capillary leakage and restoration of lymphocyte egress by a chiral S1P1 antagonist *in vivo*. *Nat Chem Biol* **2:** 434–441

Schumann K, Lammermann T, Bruckner M, Legler DF, Polleux J, Spatz JP, Schuler G, Forster R, Lutz MB, Sorokin L, Sixt M (2010) Immobilized chemokine fields and soluble chemokine gradients cooperatively shape migration patterns of dendritic cells. *Immunity* **32:** 703–713

Shulman Z, Shinder V, Klein E, Grabovsky V, Yeger O, Geron E, Montresor A, Bolomini-Vittori M, Feigelson SW, Kirchhausen T, Laudanna C, Shakhar G, Alon R (2009) Lymphocyte crawling and transendothelial migration require chemokine triggering of high-affinity LFA-1 integrin. *Immunity* **30:** 384–396

Sinha RK, Park C, Hwang IY, Davis MD, Kehrl JH (2009) B lymphocytes exit lymph nodes through cortical lymphatic sinusoids by a mechanism independent of sphingosine-1-phosphate-mediated chemotaxis. *Immunity* **30:** 434–446

Sixt M, Kanazawa N, Selg M, Samson T, Roos G, Reinhardt DP, Pabst R, Lutz MB, Sorokin L (2005) The conduit system transports soluble antigens from the afferent lymph to resident dendritic cells in the T cell area of the lymph node. *Immunity* **22:** 19–29

Smith ME, Ford WL (1983) The recirculating lymphocyte pool of the rat: a systematic description of the migratory behaviour of recirculating lymphocytes. *Immunology* **49:** 83–94

Svensson L, Howarth K, McDowall A, Patzak I, Evans R, Ussar S, Moser M, Metin A, Fried M, Tomlinson I, Hogg N (2009) Leukocyte adhesion deficiency-III is caused by mutations in KINDLIN3 affecting integrin activation. *Nat Med* **15:** 306–312

Tal O, Lim HY, Gurevich I, Milo I, Shipony Z, Ng LG, Angeli V, Shakhar G (2011) DC mobilization from the skin requires docking to immobilized CCL21 on lymphatic endothelium and intralymphatic crawling. *J Exp Med* **208:** 2141–2153

Tomura M, Yoshida N, Tanaka J, Karasawa S, Miwa Y, Miyawaki A, Kanagawa O (2008) Monitoring cellular movement *in vivo* with photoconvertible fluorescence protein "Kaede" transgenic mice. *Proc Natl Acad Sci USA* **105:** 10871–10876

von Andrian UH, Mempel TR (2003) Homing and cellular traffic in lymph nodes. *Nat Rev Immunol* **3:** 867–878

Wei SH, Rosen H, Matheu MP, Sanna MG, Wang SK, Jo E, Wong CH, Parker I, Cahalan MD (2005) Sphingosine 1-phosphate type 1 receptor agonism inhibits transendothelial migration of medullary T cells to lymphatic sinuses. *Nat Immunol* **6:** 1228–1235

Westermann J, Bode U, Sahle A, Speck U, Karin N, Bell EB, Kalies K, Gebert A (2005) Naive, effector, and memory T lymphocytes efficiently scan dendritic cells *in vivo*: contact frequency in T cell zones of secondary lymphoid organs does not depend on LFA-1 expression and facilitates survival of effector T cells. *J Immunol* **174:** 2517–2524

Woolf E, Grigorova I, Sagiv A, Grabovsky V, Feigelson SW, Shulman Z, Hartmann T, Sixt M, Cyster JG, Alon R (2007) Lymph node chemokines promote sustained T lymphocyte motility without triggering stable integrin adhesiveness in the absence of shear forces. *Nat Immunol* **8:** 1076–1085